

# Investigation of the effects of valve closing in a static expansion system

Th. Bock<sup>a,\*</sup>, M. Bernien<sup>a</sup>, Ch. Buchmann<sup>a</sup>, T. Rubin<sup>a</sup>, K. Jousten<sup>a</sup>

<sup>a</sup>*Physikalisch-Technische Bundesanstalt, Abbestraße 2–12, 10587 Berlin, Germany*

## Abstract

The precise measurement of the pressure of the gas enclosed in the starting volume of a static expansion system is important for achieving low measurement uncertainties. This work focuses on the valve closing process and the resulting pressure difference. The condition of flow conservation is used to set up a model and an experimental procedure has been developed to investigate the pressure change caused by the moving valve plate. Various parameters are evaluated and compared with experimental data.

*Keywords:* Vacuum, static expansion system, metrology, instrumentation, valve, volume, conductance

## 1. Introduction

To this day static expansion systems are one of the most accurate realizations of the pressure scale in the range from  $1 \times 10^{-2}$  Pa to 100 Pa and are used as primary standards in many metrology institutes [1]. Many contributions to the uncertainty have been investigated in great detail, e.g., the impact of the temperature during expansion and real gas effects [4, 5]. In this study we focus on the dynamic effects during the closing process of the valve that encloses the gas to be expanded. These effects become increasingly important when working with small volumes.

The PTB vacuum group currently evaluates the new static expansion primary standard SE3. SE3 will be a fully automated calibration facility for the realization and dissemination of pressures in the range  $1 \times 10^{-2}$  Pa to 100 Pa. Six DN16CF valves described in this paper are used for three starting volumes with nominal volumes of 0.02l, 0.2l and 2l. The calibration vessel has a volume of 200l. The entire calibration pressure range will be covered by three different single stage expansions. This is beneficial since multiple consecutive expansions lead to increased uncertainties. The principle of static expansion [7] relies on the transfer of a fixed amount of gas from a small volume into a larger volume. If the initial pressure and the ratio of the two volumes is known precisely, a well-known lower pressure is generated. In order to generate a calibration pressure of  $1 \times 10^{-2}$  Pa an expansion ratio  $f = V_s / (V_s + V_e)$  of  $1 \times 10^{-4}$  and a filling pressure  $p_{\text{fill}}$  of 100 Pa is used.  $V_s = 0.02$ l is the smallest starting volume of SE3.  $V_e$  is the 200l volume of the calibration vessel. The generated pressure  $p_{\text{after}}$  is obtained using the ideal gas law and the

condition that the amount of gas is constant:

$$\begin{aligned} \frac{V_s p_{\text{before}}}{T_{\text{before}}} &= N k_B = \frac{(V_s + V_e) p_{\text{after}}}{T_{\text{after}}} & (1) \\ \Rightarrow p_{\text{after}} &= p_{\text{before}} \frac{V_s}{V_s + V_e} \frac{T_{\text{after}}}{T_{\text{before}}} = (p_{\text{fill}} + \Delta p) f \frac{T_{\text{after}}}{T_{\text{before}}} \\ &= p_{\text{fill}} \left( 1 + \frac{\Delta p}{p_{\text{fill}}} \right) f \frac{T_{\text{after}}}{T_{\text{before}}} & (2) \end{aligned}$$

with  $k_B$  the Boltzmann constant,  $N$  the number of gas molecules,  $p_{\text{before}}$  the pressure and  $T_{\text{before}}$  the temperature of the enclosed gas before expansion as well as  $T_{\text{after}}$  the temperature of the gas after expansion. The filling pressure  $p_{\text{fill}}$  can only be measured outside the starting volume since a gauge introduces heat and additional volume.  $\Delta p$  denotes a potential pressure difference between the position of the gauge and inside of the closed starting volume. This pressure difference is the main topic of this work.

After presenting an initial investigation, the layout and the design of the starting volumes as well as the associated valves are described in the following. Then the pressure change during the closing phase is modeled. The derived dependencies are compared to experimental results. The experiments were performed with two different valves of the same type. Expansion ratio measurements with nitrogen, helium and argon are presented. A correction factor and an additional measurement uncertainty are introduced.

## 2. Initial investigation

To check for pressure differences due to valve closing of the starting volume, initial investigations with two pneumatic DN16CF all-metal angle valves of the type VAT 57124-GE44-0002 and VAT F57-74423-02 were conducted. The latter is modified: it has a reduced closing path of 2 mm and is used on the primary standard SE1

\*Corresponding author

Email addresses: thomas.bock@ptb.de (Th. Bock), matthias.bernien@ptb.de (M. Bernien), christian.buchmann@ptb.de (Ch. Buchmann), tom.rubin@ptb.de (T. Rubin), karl.jousten@ptb.de (K. Jousten)

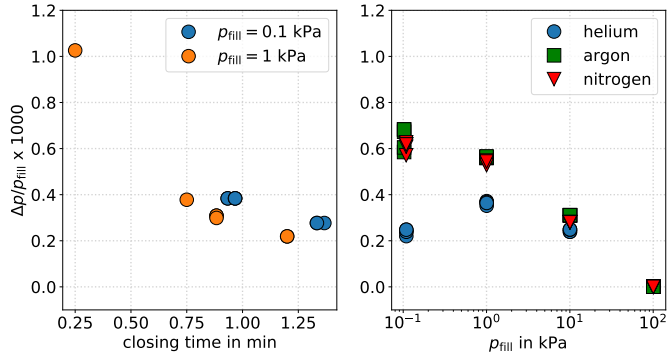


Figure 1: Results of initial investigations with a pneumatic DN16CF angle valve of the type *VAT 57124-GE44-0002* and an experimental setup as shown in Figure 5. The relative pressure differences across the valve plate after the closing process are plotted as a function of closing time for two different filling pressures of helium (left) and as a function of filling pressure for helium, argon and nitrogen with a closing time of 1 min (right). The volume enclosed by the valve was about  $30 \text{ cm}^3$ . The closing time was varied via a throttle and relates here to the entire valve stroke of about 7 mm. 1 min closing time corresponds to a closing speed of about  $120 \mu\text{m/s}$ .

[2, 3]. Figure 1 shows results with the valves of the first type. A differential capacitance diaphragm gauge (CDG) was used to measure  $\Delta p$  after closing the valve while varying the filling pressure, closing speed and gas species (see Figure 5). The experiments show that after the valve's closing position was reached a constant pressure indication remains. Relative differences up to  $1 \times 10^{-3}$  occur at high closing speeds. Varying the filling pressure causes relative differences up to  $7 \times 10^{-4}$ , depending on the gas species. It became obvious that these deviations would significantly increase the measurement uncertainty of the system. To gain a better understanding, time resolved experiments were carried out as described below. The use of servomotors allows for a precise speed and force control of the valve closing process.

### 3. Valves of the starting volume

Each of the starting volumes of SE3 consists of an aluminum cylinder and two DN16CF valves (inlet and outlet valves). The aluminum cylinders are designed and build to ensure an easily measurable volume. With a nominal volume of  $5 \text{ cm}^3$  the valves contribute with 50% to the value of  $V_s$ . The inlet and the outlet valves used for  $V_s$  are DN16CF all-metal angle valves of the manufacturer VAT (Type 571 24-GE02). A schematic drawing of the valves is shown in Figure 2. The valve plate is a sealing ring mounted to a piston with a bellows as a flexible element that is mechanically coupled to a threaded rod. Upon rotation the threaded rod moves forward in a hollow shaft. When reaching the closing position the sealing ring seals against the valve seat and the piston. The force acting on the sealing ring is lifting the hollow shaft and transferred to plate springs that provide a well-defined closing force.

### 3.1. Geometrical dimensions

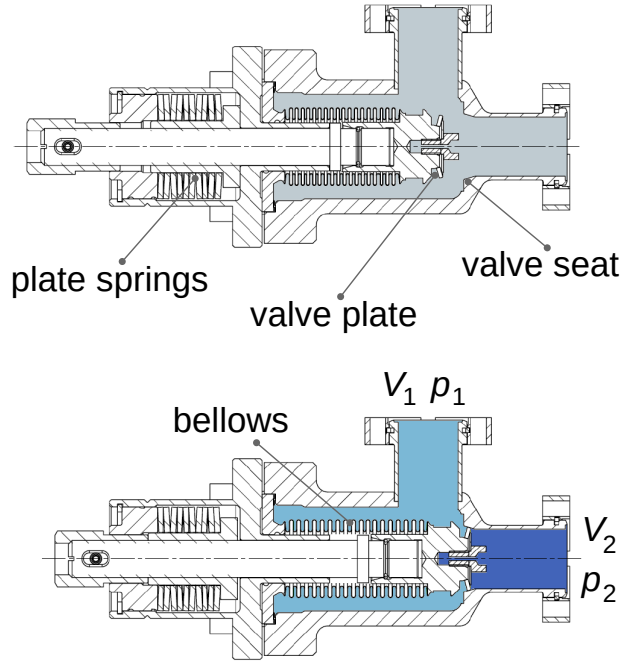


Figure 2: Schematic drawing of the valve closing mechanism.

For the purpose of the geometric determination of the contributing volume three valves were characterized by means of a 3D coordinate measuring machine. The dimensions of the inner volume were measured with up to 10  $(x, y, z)$ -line-scans per valve. These scans were used to create the schema in Figure 3.

From these measurements a model of the valve with mean coordinates and uncertainties is derived. The sealing point of this model valve is determined to be at a radius of  $(8.46 \pm 0.01) \text{ mm}$  and the slope of the valve seat is  $m_{\text{seat}} = -(0.267 \pm 0.002) \text{ mm/mm}$ . The radius of the valve plate is about 8 mm, its length together with its support almost 25 mm. The valve seat is 3 mm long.

### 3.2. Valves closing mechanism

Servomotors are used to open and close the valves. They provide a more precise control of the valve plate position, velocity and closing torque compared to a pneumatic setup. The motors are coupled to a gear with a ratio of  $R = 1/169$ . The spindles of the valves have a pitch of  $s = 1.4 \text{ mm}$  per revolution. The linear velocity of the piston of the valve formed by the valve plate together with the valve bellows is given by

$$v = \omega R s \quad (3)$$

where  $\omega$  is the number of revolutions per minute. The relevant rotational speed range lies between  $\omega = 20 \text{ rpm}$  and  $\omega = 100 \text{ rpm}$ . With Equation 3 one gets velocities  $v$  between  $2.8 \times 10^{-6} \text{ m/s}$  and  $14 \times 10^{-6} \text{ m/s}$ .

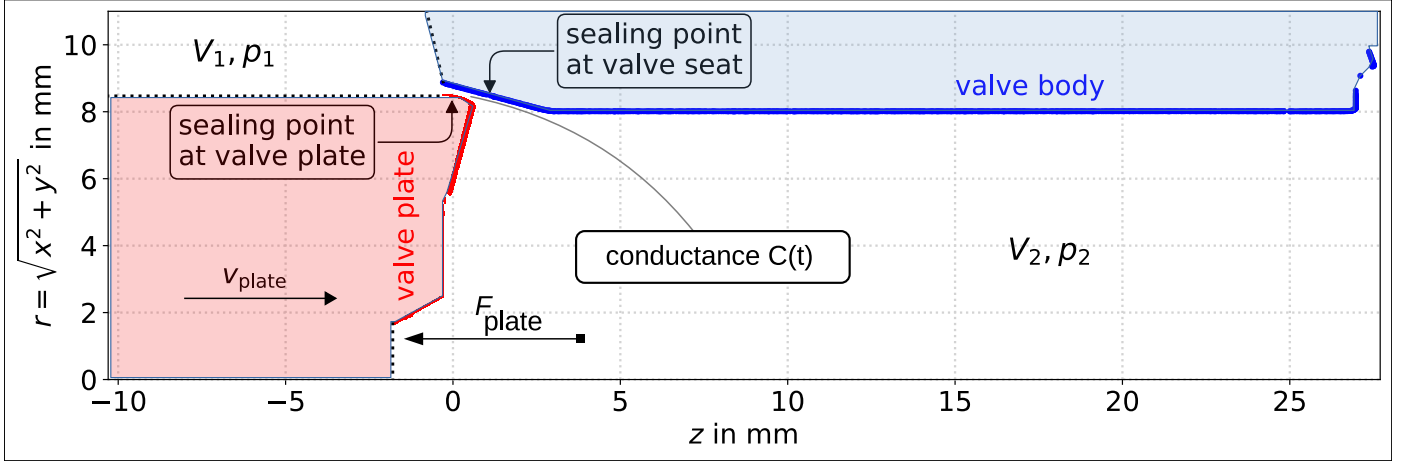


Figure 3: Scans along the inlet valve body (blue) and the valve plate (red). Until the valve is closed, the volumes  $V_1$  and  $V_2$  are connected via the conductance  $C(t)$ . In the diagram the valve plate is positioned  $\approx 1$  mm in front of the closed position. The direction of movement and the speed of the valve plate during the closing process are indicated by an arrow. The factor  $g_{\text{spring}}$  is equal to 1 as long as there are no forces in  $z$  direction. Furthermore,  $F_{\text{plate}}$ , the position of the sealing point at the valve plate and at the valve body is annotated.

The regulation circuit of the servomotor control is used to force a constant rotation velocity. To keep  $\omega$  constant, the servomotor current  $i_{\text{servo}}$  increases with increasing torque. The motor is stopped when the spring socket reaches its stopper and specified torque for closing the valve is reached.

### 3.3. Valve spring

The valve's closing mechanism includes an arrangement of plate springs. If a force  $F_{\text{plate}}$  is exerted on the valve plate, the spring structure is deformed according to Hook's law by  $\Delta z = \frac{F_{\text{plate}}}{D}$  where  $D$  is the spring constant and  $\Delta z$  the length difference due to deformation. The plate springs have a spring constant  $D$  of 2400 N/mm and are pre-loaded with a force  $F_{\text{plate}}$  of about 600 N corresponding to a deformation  $\Delta z$  of about 0.25 mm. Once the valve plate reaches the sealing point, the force on the valve plate increases. When the force exceeds the pre-load, the deformation of the plate springs increases according to  $\Delta \dot{z} = \Delta v = \frac{\dot{F}_{\text{plate}}}{D}$ . Consequently, the relation between  $\omega$  and  $v$  as given in Equation 3 is modified. For  $\dot{F}_{\text{plate}} > 0$ , the velocity of the valve plate  $v_{\text{plate}} = v - \Delta v$  is reduced. This is accounted for by a factor  $g_{\text{spring}} = 1 - \frac{\Delta v}{v}$ , hence

$$v_{\text{plate}} = \omega R s g_{\text{spring}}. \quad (4)$$

## 4. Model of gas flow during valve closing

The pressure and flow conditions during the closing process can be modeled by means of two coupled differential equations

$$V_1 \frac{dp_1}{dt} = -p_1 \frac{dV_1}{dt} + C(t)(p_2 - p_1) \quad (5)$$

and

$$V_2 \frac{dp_2}{dt} = -p_2 \frac{dV_2}{dt} - C(t)(p_2 - p_1) \quad (6)$$

based on the condition of flow conservation and the definition of flow conductance. The temperature is assumed to be constant. Here,  $C(t)$  is the time-dependent conductance formed by the gap between valve plate and valve body.  $V_1$  and  $p_1$  denote the volume and the pressure behind the valve plate (left in Figures 2 and 3).  $V_2$  and  $p_2$  are the starting volume and the pressure of the enclosed gas in front of the valve plate (right in the Figures 2 and 3). The pressure  $p_1$  is measured by means of a Quartz Bourdon Spiral during the initial experiments. At the later experiments  $p_1$  is measured by means of a group of 15 capacitance diaphragm gauges (SE3 group standard).  $p_1$  corresponds to the filling pressure  $p_{\text{fill}}$  introduced in Equation 2.

During the experiments and during a calibration the inlet valve is closed and afterwards  $p_{\text{fill}}$  is measured. The metrologically relevant but inaccessible quantity is the pressure  $p_2 = p_{\text{fill}} + \Delta p$ . Equation 6 can be rewritten as

$$\dot{p}_2 = \frac{1}{V_2} \left( -p_2 \dot{V}_2 - C(t) \Delta p(t) \right). \quad (7)$$

The following sections present information on  $p_2 \dot{V}_2$  called the *volume term* and  $C(t) \Delta p(t)$  named *conductance term*.

### 4.1. Volume term

The term  $p_2 \dot{V}_2$  corresponds to a flow caused by the motion of the valve plate along the  $z$  axis at a pressure  $p_2$ . With an area of  $A_{\text{plate}} = \pi r_{\text{plate}}^2$  the volume term can be expressed by the equation  $p_2 \dot{V}_2 = p_2 \frac{A_{\text{plate}} dz}{dt} = p_2 A_{\text{plate}} v g_{\text{spring}}$ . Table 1 gives an overview for the case  $g_{\text{spring}} = 1$  and a volume of  $V_2 = 0.021$ .

The volume term increases the pressure in  $V_2$ . It is independent of the gas species and countered by the conductance term when  $\Delta p(t) > 0$ .

Table 1: Selected values of the volume term  $p_2 \dot{V}_2$  for  $V_2 = V_s = 0.021$ .

$\omega$ in rpm	$-\dot{V}_2$ in $\text{cm}^3/\text{s}$	$-\dot{V}_2/V_s$ in $1/\text{s}$
20	$6.3 \times 10^{-4}$	$3 \times 10^{-5}$
80	$2.5 \times 10^{-3}$	$1.3 \times 10^{-4}$
100	$3.1 \times 10^{-3}$	$1.6 \times 10^{-4}$

#### 4.2. Conductance term

The conductance  $C(t)$  strongly depends on the position  $z(t)$  of the valve plate relative to the valve body. Before entering the conical section of the valve seat (see Figures 2 and 3) no significant pressure difference  $\Delta p(t) = p_2 - p_1$  is possible because of the large gap between valve plate and valve body. In this range the molecular flow conductance is about  $51/\text{s}$  and the viscous conduction is even higher. Due to the conical shape of the valve body,  $C(t)$  decreases until the sealing point is reached. For the position of the valve plate sketched in Figure 3 the gap is about  $\Delta r = 0.27$  mm.

In the molecular regime, the conductance of an annular gap with inner radius  $r_i$ , outer radius  $r_o$  and length  $l$  is given by [6]:

$$C_{\text{mol}} = \sqrt{\frac{RT}{2\pi M}} \pi (r_o^2 - r_i^2) \left( \frac{\frac{3l}{\Delta r} + \frac{l}{\Delta r + l/7}}{\frac{16}{\pi} \ln(4\alpha + \frac{r_i/r_o + 0.81}{\alpha})} + 1 \right)^{-1}, \quad (8)$$

$$\alpha = \left( 1 + \beta \frac{l}{2\Delta r + l} \frac{r_i}{r_o} - \left( \frac{l}{2\Delta r + l} \frac{r_i}{r_o} \right)^{(1 + \frac{r_i}{r_o})} \right)^{-\frac{1}{2}}$$

where  $R$  is the gas constant,  $T$  the temperature of the gas,  $M$  the molar mass of the gas molecules and  $\beta = 0.0225$  if  $r_i/r_o < 0.99$ , otherwise  $\beta = 0.225\sqrt{1 - r_i/r_o}$ . The inner radius of the annular gap can be identified with the radius of the valve plate:  $r_i = r_{\text{plate}}$ . The outer radius is given by the radius of the valve seat that depends on the position of the valve plate. Until the sealing point at  $z = 1$  mm is reached, the outer radius is given by  $r_o = r_i + m_{\text{seat}}(1 \text{ mm} - z)$ . Equation 8 is valid for the molecular flow regime. At the lowest filling pressure of 100 Pa, the mean free path is  $\lambda = 66 \mu\text{m}$  for nitrogen corresponding to a Knudsen number of  $Kn = \lambda/d_h = 1.2$  at  $z = 0.9$  mm, with the hydraulic diameter of an annular gap given as  $d_h = 2\Delta r$ . If the valve plate continues to move along the  $z$ -axis,  $\Delta r$  decreases and  $Kn$  increases. On the other hand, with increasing filling pressure  $Kn$  decreases such that the assumption of molecular flow is not valid. In the viscous regime and laminar flow conditions, the conductance of an annular gap is given by [7]:

$$C_{\text{vis}} = \frac{\pi}{16\eta l} \left( r_o^4 - r_i^4 + \frac{(r_o^2 - r_i^2)^2}{\ln(r_i/r_o)} \right) (p_1 + p_2) \quad (9)$$

with  $\eta$  the viscosity of the gas. Note that due to  $p_1/p_2 \approx 1$  no choking of the gas flow occurs. Hence, the conductance

strongly increases with increasing pressure. The conductance over the entire pressure range is given by [6]:

$$C_{\text{gap}} = C_{\text{vis}} + \frac{C_{\text{mol}}}{1 + \frac{3\pi}{128} \frac{1}{Kn} \left( 1 - \left( 1 - \frac{(1+4Kn)Kn^{0.45}}{1+Kn} \right) \frac{l}{l+d_h} \right)} \quad (10)$$

Interestingly, the strong increase in conductance in the viscous regime only leads to moderate reduction in the relative pressure difference of about 33% for a filling pressure of 100 Pa and 100000 Pa as shown in Figure 12a. The reason is that only close to the sealing point a significant pressure difference builds up and that  $C_{\text{gap}}$  asymptotically approaches  $C_{\text{mol}}$  when  $r_o$  approaches  $r_i$ .

Table 2: Estimation of the conductance in the molecular regime at room temperature and nitrogen for an annular gap with length  $l = 0.2$  mm according to Equation 8.  $z$  is given relative to the position shown in Figure 3.

$z$ in mm	$\Delta r$ in mm	$C_{\text{mol}}$ in $\text{cm}^3/\text{s}$
0	0.267	1290
0.9	0.0267	48
0.99	0.00267	1.0

Beside the pressure dependency,  $C(t)$  also depends on the gas species. This affects  $p_2$  via Equation 7 and therefore the amount of gas enclosed in the starting volume once the valve is closed.

#### 4.3. Pressure change

The time-dependent pressure change can be obtained by numerical solution of Equations 5 and 6 with  $C(t)$  from Equations 8 to 10. The change in volume is solely attributed to  $V_2$ , and  $\dot{V}_1$  is set to zero. Other choices are possible but will not affect the result because a significant pressure difference only builds up shortly before the closing position of the valve plate is reached.

Figure 4 shows the calculated time-dependent change of the starting volume (a), flow conductance (b), pressures (c) and relative pressure difference (d) for  $\omega = 80$  rpm,  $g_{\text{spring}} = 0.02$ ,  $V_1 = 31$  and nitrogen. Four positions of the valve plate at  $z = 0.90, 1.00, 1.01$  and  $1.02$  mm are indicated by vertical lines. The first line marks the position at which a significant pressure difference builds up. The second line marks the position at which the valve plate starts to seal against the valve seat and the velocity of the valve plate is strongly reduced to  $vg_{\text{spring}}$ . The third line marks the positions up to which a potential leak after sealing against the valve seat persists. The last line marks the position at which the specified closing torque of the valve is reached and the movement of the valve plate is stopped.

In Figure 4c the pressure in the starting volume  $p_2$  (yellow) and in the volume of the gas inlet  $p_1$  (blue) are plotted as a function of time together with the pressure change for a situation in which a leak of  $0.2 \text{ cm}^3/\text{s}$  persists up to

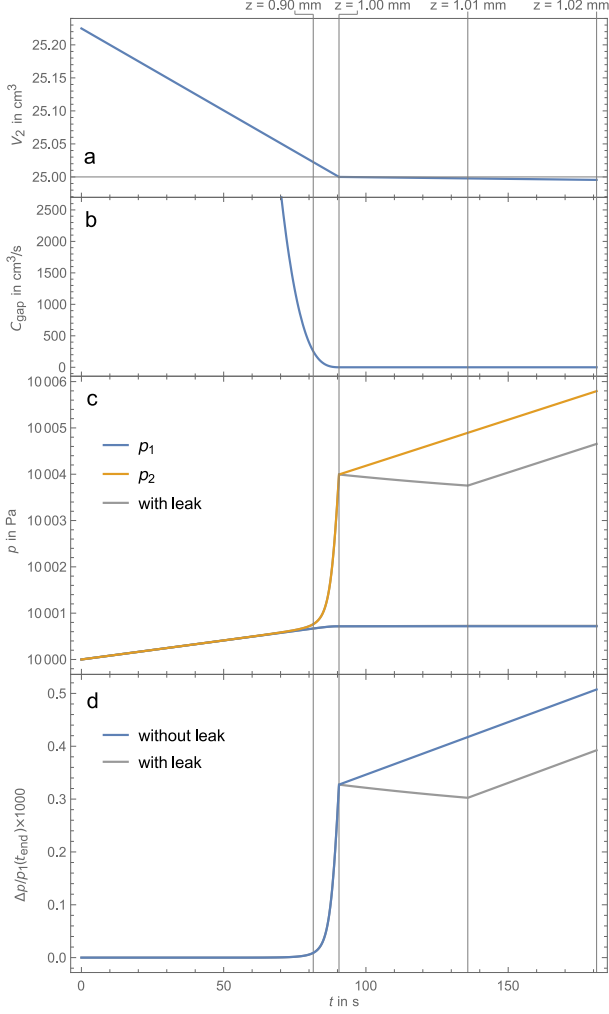


Figure 4: Calculated time dependence of the starting volume (a), flow conductance (b), pressures (c) and relative pressure difference (d) for  $\omega = 80$  rpm,  $g_{\text{spring}} = 0.02$ ,  $V_1 = 3l$  and nitrogen. Four positions of the valve plate at  $z = 0.90, 1.00, 1.01$  and  $1.02$  mm are indicated by vertical lines. A horizontal line in panel (a) highlights that after reaching  $z = 1.00$  mm the change in  $V_2$  is strongly reduced but not zero.

$z = 1.01$  mm. Four different phases of the valve-closing process can be identified. Up to about  $z = 0.90$  mm, the change in volume is constant and causes a relative change in pressure according to  $\dot{p}_1/p_1 = \dot{p}_2/p_2 = -\dot{V}_2/(V_1 + V_2)$ . The flow conductance is decreasing but no significant pressure difference is generated down to about  $300 \text{ cm}^3/\text{s}$  (see Figure 4b and 4d). Below this conductance, the pressure in the starting volume rises strongly approaching  $\dot{p}_2/p_2 = -\dot{V}_2/V_2$ . When the valve plate reaches the sealing point ( $z = 1.00$  mm) its movement is strongly reduced because of the force exerted. The change in pressure in the starting volume is now  $\dot{p}_2/p_2 = -g_{\text{spring}}\dot{V}_2/V_2$ . The increase in pressure maybe partly counteracted by a gas flow through a leak until the valve is fully sealed at  $z = 1.01$  mm (gray lines in Figure 4c and d). The pressure in the starting volume continues to increase until the closing torque is

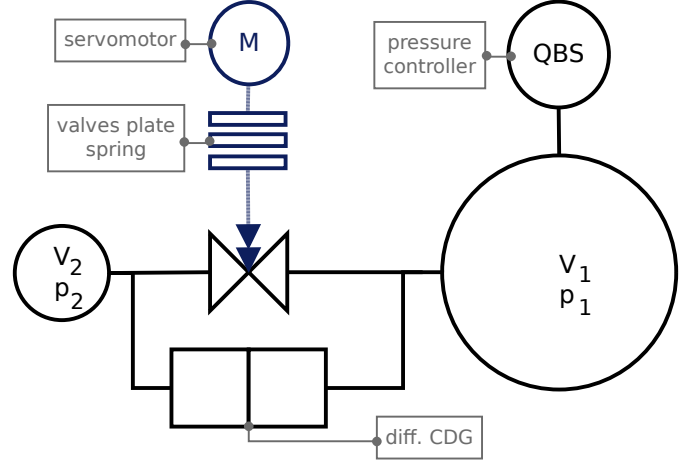


Figure 5: Experimental setup. A Quartz Bourdon Spiral (QBS) was used to set and measure the pressure  $p$ . During the valve closing process the differential pressure  $\Delta p(t)$  across the valve plate as well as the servomotor current  $i_{\text{servo}}$  are recorded. The experiment was realized with two different valves of the same model.

reached and the movement of the valve plate is stopped ( $z = 1.02$  mm). The model contains four valve-specific parameters that must be adjusted to match the measurements: the reduction in movement of the valve plate  $g_{\text{spring}}$  once the sealing point is reached, the position at which the closing torque is reached, the size of a potential leak, and the length of the channel of the annular conductance formed by the valve plate and the seat. The latter significantly impacts the pressure difference that is built up in the moment the sealing position is reached and is chosen to be  $0.2$  mm here.

## 5. Experiment

The differential pressures were investigated systematically by varying the parameters  $V_1$ ,  $V_2$ ,  $\omega$ ,  $p_1$  and the gas species. Figure 5 shows a sketch of the experimental setup.  $\Delta p(t)$  was measured by means of a differential capacitance diaphragm gauge with a full scale of  $1.3$  kPa. The heater of the CDG was turned off. For each measurement run, the valve plate was set about  $2$  mm in front of the closing position, where the offset corrected signal of the CDG is still zero. Then the closing process was initiated and the CDG measurement signal was recorded as a function of time until the closing torque was reached. In some cases the current consumption of the servomotor was recorded simultaneously. The measurements were repeated several times in order to examine the repeatability.

All measurements show more or less the characteristics plotted in Figure 6. The graph can be roughly separated in two parts. Up to the position marked with (A), the slope of the relative pressure change  $r_p = \frac{\Delta p(t)}{p_1}$  depends on the volume  $V_2$ . Beside the closing speed dependency the height of  $r_p$  corresponds to the travel length, the valve

plate can move without an occurring  $F_{\text{plate}}$  in the region with low conductivity. After the position marked with (A), the slope of  $r_p$  depends mainly on the valve spring constant  $D$ .

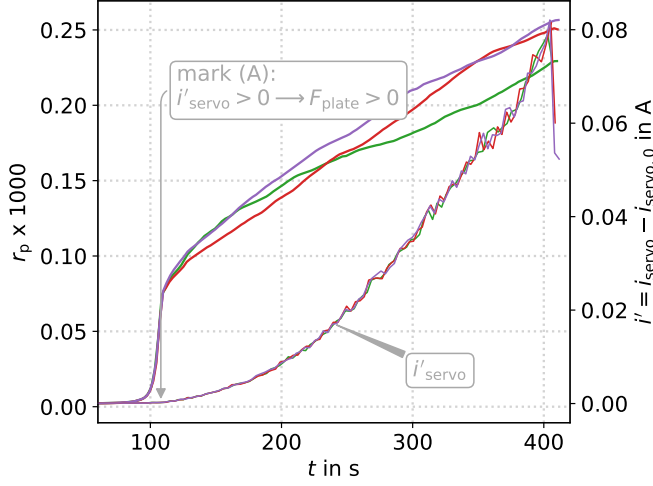


Figure 6: Three repeated measurements of the servomotor current  $i'$  (axis on the right) and the relative pressure difference  $r_p$  (axis on the left) at  $\omega = 20$  rpm,  $V_1 = 31$  and a volume  $V_2 = 25$  ml. The ripples in the current tracks may point to a discontinuous movement of the valve plate.

Figure 6 shows  $r_p$  and the current  $i' = i_{\text{servo}} - i_{\text{servo},0}$  for three repeated measurements.  $i_{\text{servo}}$  denotes the total current consumption of the servomotor and  $i_{\text{servo},0}$  the current for  $F_{\text{plate}} = 0$ .  $r_p$  and  $i_{\text{servo}}$  are simultaneously recorded. At mark (A)  $i'$  rises significantly. This can be related to the increase of the force on the valve plate by friction and an associated torque  $\tau_{\text{servo}}$ :  $F_{\text{plate}} \propto \tau_{\text{servo}} \propto i'$ . The spring deforms and the velocity of the valve plate is strongly reduced (see section 3.3). The contribution of the volume term is reduced by the same factor which results in a slope with a smaller value in the  $\Delta p(t)/p_1$  vs.  $t$  chart.

### 5.1. Volume variation

Equation 7 shows that  $\dot{p}_2 \propto \frac{1}{V_2}$ . This dependency is confirmed by the experimental results shown in Figure 7. Both series of measurements with three repetitions show the expected dependency in the slope of the resulting  $r_p$ . The diagram includes the theoretical values for the contribution of the *volume term* for the case  $V_2 = 15$  ml and  $V_2 = 25$  ml without the *conductance term*. Due to the omitted  $C(t) \Delta p(t)$  part the theoretical slopes are larger compared to the measured slopes.

The measurements shown in Figure 9 aimed also on the examination of the influence of  $V_1$  on  $p_1$ .  $V_1$  has no measurable influence on  $\Delta p(t)$  at least in the case  $V_1 \gg V_2$ .

### 5.2. Closing speed variation

The influence of the closing speed  $\omega$  was examined by the measurements plotted in Figure 8. The conductance term

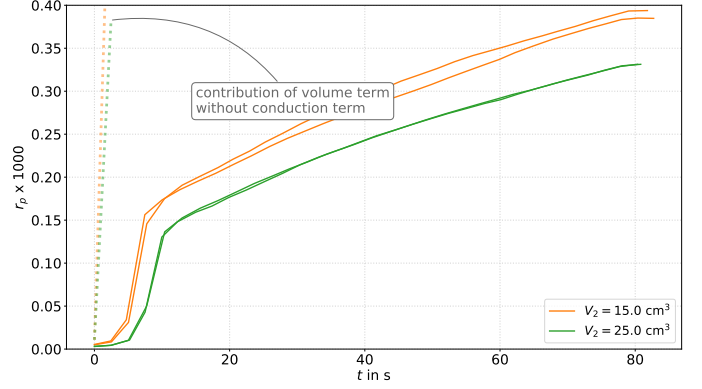


Figure 7: Relative pressure difference as a function of time for two different volumes  $V_2$  with  $p_1 = 100$  kPa,  $V_1 = 31$  and  $\omega = 100$  rpm

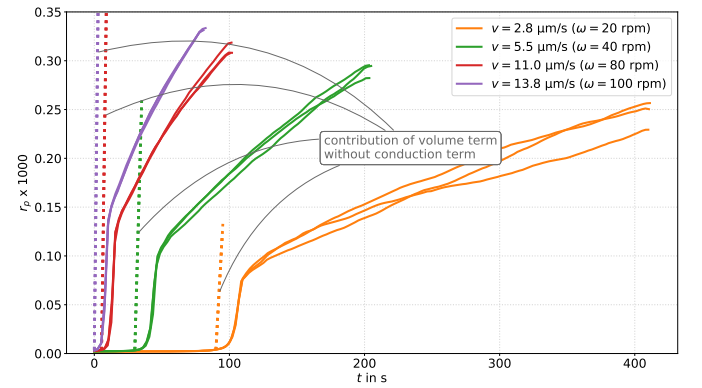


Figure 8: Relative pressure difference as a function of time for different closing speeds with  $p_1 = 10$  kPa,  $V_1 = 31$  and  $V_2 = 25$  ml

causes a back flow  $\Delta p_{\text{bf}}(t) = \int_{t_0}^t C(t') \Delta p(t') dt'$ . This means that the longer the closing process lasts the more the pressure rise in  $V_2$  is reduced by the conductance term. Like in Figure 7 the theoretical values for the contribution of the *volume term* for the case  $V_2 = 25$  ml without the  $C(t) \Delta p(t)$  part are included.

### 5.3. Influence of valve tolerances

The data shown in Figure 9 were measured using another valve of the same type as the one used for Figures 7 and 8. A different shape and height of the  $r_p$  graph can be observed. Especially the constant or partially decreasing pressure in the range 30 s to 60 s is remarkable. An explanation may be a slowed down movement of the valve plate along the  $z$ -axis or a leak that persists until the valve is fully sealed as depicted in Figure 4d. During the period when the movement stops or slows down, the conductance term lowers the  $\Delta p(t)$ .

### 5.4. Pressure variation

The influence of  $p_1$  on  $\Delta p(t)$  in Figure 9 is expected from the considerations given in section 4.2: in the viscous flow regime an increasing pressure causes an increasing

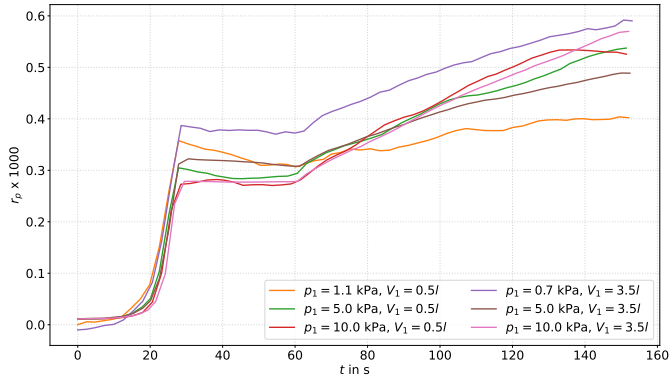


Figure 9: Relative pressure difference as a function of time for different volumes  $V_1$  and pressures  $p_1$  with  $V_2 = 25$  ml and  $\omega = 80$  rpm

conductance. With a larger  $C$  the amount of back flow from  $V_2$  to  $V_1$  becomes bigger and the pressure increase in  $V_2$  is reduced more strongly (see Equation 7).

### 5.5. Influence of the gas species on the expansion ratio

$C$  depends on the gas species. In the molecular regime  $C \propto 1/\sqrt{M}$  where  $M$  is the molar mass. Under laminar flow conditions  $C \propto 1/\eta$  where  $\eta$  is the viscosity of the gas. The effective expansion ratio of SE3 starting from  $V_s$  was determined for different gas species.  $f_{\text{eff},s}$  is determined from the pressure ratio:

$$f_{\text{eff}} = \frac{p'_{\text{after}} T'_{\text{before}}}{p'_{\text{fill}} T'_{\text{after}}} . \quad (11)$$

as shown in [9]. In Equation 11  $p'_{\text{fill}}$ ,  $T'_{\text{before}}$ ,  $p'_{\text{after}}$  and  $T'_{\text{after}}$  are the pressures and temperatures before and after the expansion at the time of determining  $f_{\text{eff}}$ .  $p'_{\text{after}}$  was measured by means of a large area non-rotating piston gauge of the type FRS5 [9] and a differential CDG.  $p'_{\text{fill}}$  was obtained by using the SE3 group standard.

For this method the following has to be considered: since  $p'_{\text{fill}}$  was measured after the closing of the inlet valve of the starting volume  $p'_{\text{before}} = p'_{\text{fill}} + \Delta p'$ . Thus,  $\Delta p'$  enlarges  $p'_{\text{after}}$  by  $2 \times 10^{-4}$  to  $6 \times 10^{-4}$  as the results of the previous section have shown. The value of the effective expansion ratio determined from a pressure ratio contains this effect: the enlarged  $p'_{\text{after}}$  causes an enlarged  $f_{\text{eff},s}$ . The subscript “eff” reflects the determination of the effective expansion ratio from a pressure ratio in contrast to the determination from a volume ratio that is referred to as  $f$ .

The largest effect of the gas species on  $f_{\text{eff}}$  is expected for the smallest volume  $V_s$ , since the volume  $V_2$  (see Equation 6) has to be small to gain a measurable effect. In order to use FRS5 for the measurement of  $p'_{\text{after}}$  with low uncertainties, the gas inside the calibration vessel has to be accumulated [8, 10]. With a filling pressure of 100 kPa and a nominal  $f_{\text{eff},s}$  of  $1 \times 10^{-4}$  one expansion step generates 10 Pa. The results of the investigation of the gas species dependency of  $f_{\text{eff},s}$  are given in Table 3.

With regard to the expansion ratios  $f_{\text{eff},s}$  measured at SE3, the differences between the values are not significant due to the measurement uncertainties.

### 5.6. Influence of closing time on calibration results

With the modified pneumatic valves of the type VAT F57-74423-02 mentioned in section 2 the experiments described in the following are carried out. The effective accommodation coefficient  $\sigma = p_{\text{ind}}/p_{\text{after}}$  of two spinning rotor gauges (SRG) [11] are determined at a pressure of  $3 \times 10^{-2}$  Pa. Here  $p_{\text{ind}}$  denotes the pressure indicated by the SRG at the pressure  $p_{\text{after}}$  generated by the primary standard SE1. The starting volume has a nominal value of 17 ml. The calibration vessel has a size of 230 l, such that the filling pressure was approximately 400 Pa. The corresponding expansion ratio  $f_{\text{eff},1}$  was determined via a pressure ratio in the same way as described in the previous section. For this determination the starting volume’s inlet valve was operated with a closing time of  $t_{\text{close}} = 30$  s. This corresponds to a closing speed of  $67 \mu\text{m/s}$ .

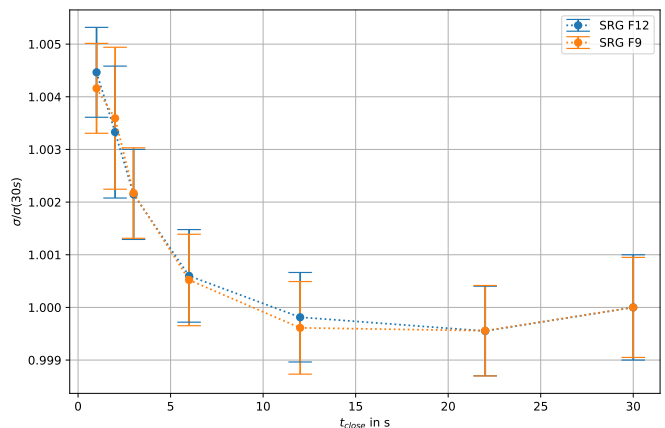


Figure 10: Influence of the variation of the closing time on calibration results of the static expansion system SE1. With the help of a throttle in the pneumatic system the closing time  $t_{\text{close}}$  was varied between 1 s and 30 s. The effective accommodation coefficients  $\sigma$  of the two SRGs (F9 and F12) are normalized to  $\sigma(30\text{s})$  since the used expansion ratio  $f_{\text{eff},1}$  was determined with  $t_{\text{close}} = 30$  s. The error bars indicate the combined Type A and Type B standard measurement uncertainty.

Figure 10 shows the calibration results for a successive reduction in closing time. The corresponding closing speeds vary between 2 mm/s and  $67 \mu\text{m/s}$ .  $t_{\text{close}}$  was changed by means of the throttle in the pneumatic system of the inlet valve. The results of Figure 10 show that differences up to 0.4% occur when the valve is closed with a speed of 2 mm/s compared to the value obtained with the speed used for the determination of  $f_{\text{eff},1}$ . These deviations are caused by the enlarged calibration pressure due to the dependence of  $r_p$  on the closing speed.

Table 3: Result of expansion ratio measurements carried out according the method described in [8, 10] and [9] for different gas species. Given are the proportional factors  $1/\sqrt{M}$  and  $1/\eta$  of the gas species. Furthermore, the determined values of  $f_{\text{eff},s}$  and the expanded relative type A measurement uncertainties with a coverage factor of  $k = 2$ .

gas	$1/\sqrt{M}$ $\text{g}^{-1/2} \text{mol}^{1/2}$	$1/\eta$ $\mu\text{Pa}^{-1} \text{s}^{-1}$	$f_{\text{eff},s}$	$u_a(f_{\text{eff},s})$
helium	$5.0 \times 10^{-1}$	$5.0 \times 10^{-2}$	$1.05723 \times 10^{-4}$	$7.2 \times 10^{-8}$
nitrogen	$1.9 \times 10^{-1}$	$5.6 \times 10^{-2}$	$1.05759 \times 10^{-4}$	$5.8 \times 10^{-8}$
argon	$1.6 \times 10^{-1}$	$4.4 \times 10^{-2}$	$1.05739 \times 10^{-4}$	$3.7 \times 10^{-8}$

## 6. Discussion

### 6.1. Temperature influence

The experiments described in section 5 were carried out in a room where the temperature changes are less than 0.15 K/h. This maximum temperature change results in a relative change in pressure of  $8 \times 10^{-6} \text{min}^{-1}$ . These variations have a random characteristics. A potential heat contribution caused by friction between the plate and the valve seat is considered to be negligibly small.

### 6.2. Influence of valve bellows volume change

The change in the volume of the valve due to deformation of its bellows (see Figure 2)  $\Delta V_{\text{bellow}}$  is negligible too: on the one hand  $\Delta V_{\text{bellow}}$  relates to the volume  $V_1 + V_2$  until  $V_1$  and  $V_2$  are separated by a low  $C$ . When  $V_1$  and  $V_2$  are separated  $\Delta V_{\text{bellow}} \ll V_1$  applies safely. At least, Figure 9 shows no indication of a significant influence of  $\Delta V_{\text{bellow}}$ .

### 6.3. Discontinuous closing movement

Figure 3 suggests that there is no contact between the valve plate and the seat until closing torque is reached. However, if the valve is open, the valve plate can be moved freely by about 1 mm to 2 mm perpendicular to the  $z$  axis. This is an intended engineering behavior since it is necessary to avoid a mechanical over determination. The observed flattening of the  $r_p$  curve in Figure 9 can be explained by a discontinuous movement in combination with a small conductance  $C$ . Moreover, Figure 6 gives indications for a stick slip motion by the  $i'_{\text{servo}}$  signal especially for small  $\omega$ . Since the stick slip friction has a random characteristic, the overall final  $\Delta p(t)$  contains some random contributions.

## 7. Implications for the generated calibration pressure

In a static expansion system, the generated pressure is obtained from the filling pressure and the expansion ratio according to Equation 2. If the expansion ratio  $f$  is determined from the absolute values of the volumes  $V_s$  and  $V_e$ , the filling pressure must be corrected by the factor

$\tilde{K} = (1 + \frac{\Delta p}{p_{\text{fill}}}) = (1 + r_p)$ . In such a situation it is advisable to ensure that  $r_p$  is minimal, e. g. by reducing the speed of the valve.

Alternatively, an effective expansion ratio  $f_{\text{eff}}$  can be determined from a measurement of a filling pressure  $p'_{\text{fill}}$  and the pressure after expansion  $p'_{\text{after}}$  as described in section 5.5. From Equation 11 and 2 it follows:

$$f_{\text{eff}} = \left(1 + \frac{\Delta p'}{p'_{\text{fill}}}\right) f \quad (12)$$

When using this method the effect of  $\Delta p$  is calibrated into  $f_{\text{eff}}$  for the conditions used during its determination. Substituting Equation 12 into Equation 2, the generated pressure is given by

$$p_{\text{after}} = p_{\text{fill}} \frac{1 + \frac{\Delta p}{p_{\text{fill}}}}{1 + \frac{\Delta p'}{p'_{\text{fill}}}} f_{\text{eff}} \frac{T_{\text{after}}}{T_{\text{before}}} \quad (13)$$

and the correction factor becomes  $K = (1 + r_p)/(1 + r'_p)$ . Thus,  $K = 1$  when the conditions during use are the same as during the determination of the effective expansion ratio.

The considerations in section 4 showed that a pressure and gas species dependence of  $r_p$  can be expected. Both dependencies are introduced by the conductance term. The closing process takes place within the viscous flow regime. Here a smaller  $p_{\text{fill}}$  causes a smaller  $C$ . A smaller molecular mass causes a larger  $C$  with a  $1/\sqrt{M}$  and a smaller viscosity causes a larger  $C$  with  $1/\eta$ . Due to the high measurement uncertainty and the small size of the effect, it was not measurable as Table 3 shows. However, a correction factor should be introduced.

### 7.1. Pressure dependent correction factor

For the calibration pressures generated by means of  $V_s = 0.021$  l a correction  $K_p$  is derived on the basis of the experimental data shown in Figure 11. Here, the maximum reached  $r_p$ , measured at a closing speed of  $\omega = 80$  rpm are plotted across the pressure  $p_{\text{fill}}$  for the volumes  $V_2 = 0.015$  l and  $V_2 = 0.025$  l.  $V_1$  lies between 0.5 l and 3.5 l. From these data the slope  $\tilde{m}$  and offset  $b$  are derived by means of a linear regression:  $r_p(p_{\text{fill}}) = \tilde{m} p_{\text{fill}} + b$ . The correction

factor is then given by

$$K_p = \frac{1 + \tilde{m} p_{\text{fill}} + b}{1 + \tilde{m} p'_{\text{fill}} + b} = 1 + m(p_{\text{fill}} - p'_{\text{fill}}) \\ = 1 - 2.4 \times 10^{-9} \text{ Pa}^{-1} (p_{\text{fill}} - 101300 \text{ Pa}) \quad (14)$$

where  $m = \tilde{m}/(1 + \tilde{m} p'_{\text{fill}} + b)$ . At 101.3 kPa, the filling pressure used to determine  $f_{\text{eff},s}$ ,  $K_p - 1$  becomes 0. For 100 Pa, the smallest  $p_{\text{fill}}$ ,  $K_p$  increase the calibration pressure by a relative value of  $2 \times 10^{-4}$ .  $K_p$  has a relative standard measurement uncertainty of  $2.3 \times 10^{-5}$ .

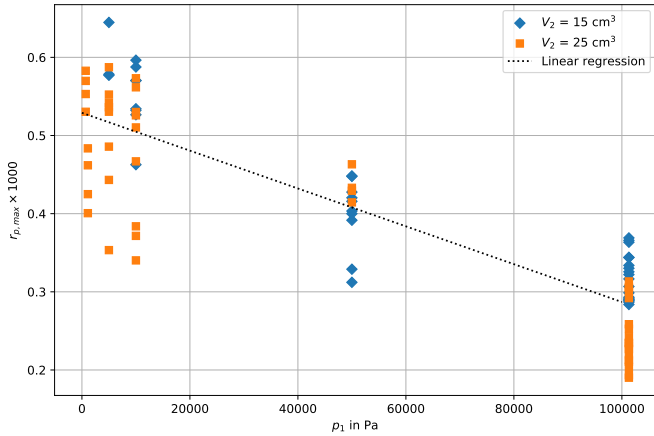


Figure 11: Experimental data for various  $V_1$ , a closing speed of  $\omega = 80$  rpm,  $V_2 = 0.0151$  and  $V_2 = 0.0251$  together with a linear regression of the data.

## 7.2. Measurement uncertainty due to gas-species dependency

Since the differences between the values of  $f_{\text{eff},s}$  for nitrogen, argon and helium are not significant (see Table 3), the dependency of  $f_{\text{eff},s}$  on the gas species will not be corrected. Instead it will be accounted for by an additional gas species and filling pressure dependent uncertainty contribution based on the numerical model introduced in section 4. In Figure 12 the relative pressure difference (a), the correction factor (b) and standard uncertainty (c) for helium and argon relative to nitrogen are shown as a function of filling pressure. The values are calculated for a valve without leak (cf. Fig. 4) and a closing speed of 80 rpm. The correction factor is calculated according to  $K_g = (1 + r_p(p_{\text{fill}}, g))/(1 + r_p(p_{\text{fill}}, \text{N}_2))$  with  $g = \text{He}, \text{Ar}$ . The contribution to the standard measurement uncertainty is estimated by  $u_g = |K_g - 1|$ .

## 8. Summary and Conclusions

Due to the valve closing process pressure differences occur depending on the volume, closing speed, filling pressures and the gas species. The effects can be described by a differential equation derived from the condition of flow

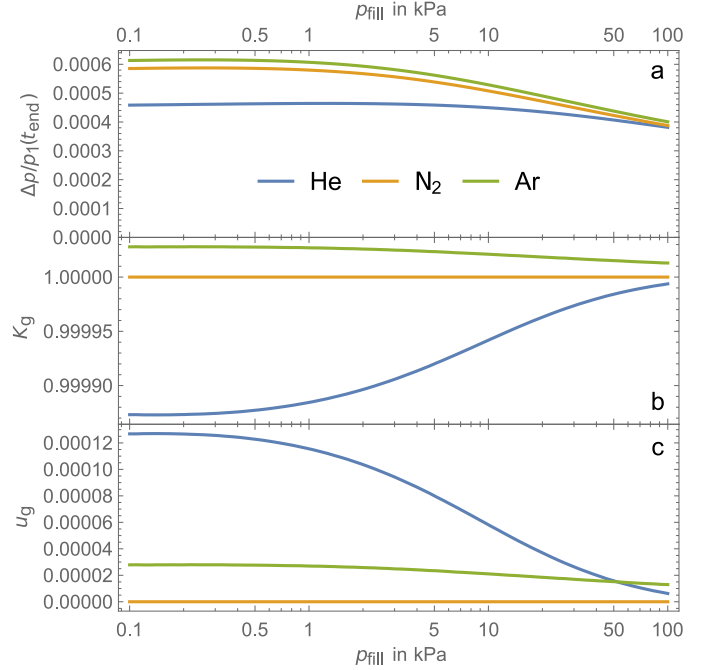


Figure 12: Relative pressure difference (a), correction factor (b) and standard uncertainty (c) for helium and argon relative to nitrogen as a function of filling pressure. The values are calculated for a valve without leak (cf. Fig. 4) and a closing speed of 80 rpm.

conservation. For a DN16CF angle valve and volumes of a size around 0.021 (size of the smallest starting volume of SE3) relative pressure differences of some  $10^{-4}$  are observed. Relative pressure differences up to  $4 \times 10^{-3}$  were observed at SE1 when operating the valve of the starting volume with full closing speed.

Since the three expansion ratios at SE3 are determined from pressure ratios which include the closing process, the effect of an enlarged gas amount is reflected in the values of  $f_{\text{eff},i}$ . It seems to be advisable to reevaluate the value of  $f_{\text{eff},i}$  if the inlet valve of the starting volume is replaced. The same valve closing speed should be used during calibrations as was used to determine  $f_{\text{eff},i}$ . The minor contribution of the filling pressure and gas-type dependencies are considered by a correction factor and by a measurement uncertainty contribution, respectively. Caution must be taken when transferring our observation to a different valve. The values we present may serve as an estimate but cannot replace an individual assessment of the valve. On the other hand, the presented methodology is generally applicable. These insights on the dynamic effects during the closing process of small volumes pave the path towards an accurate assessment of enclosed amounts of gas most relevant but not limited to the application in static expansion systems.

## Acknowledgment

Kurt Sonderegger from VAT Group AG is acknowledged for the insights he provided on the mechanical design of the valve.

## References

- [1] J. Ricker, J. Hendricks, Th. Bock, P. Dominik, T. Kobata, J. Torres and I. Sadkovskaya, Final report on the key comparison CCM.P-K4.2012 in absolute pressure from 1 Pa to 10 kPa, *Metrologia*, 54 (2017), Tech. Suppl., doi: 10.1088/0026-1394/54/1A/07002
- [2] K. Jousten and G. Rupschus, The uncertainties of calibration pressures at PTB, *Vacuum* 44 (1993), 569–572.
- [3] K. Jousten, P. Röhl and V. A. Contreras, Volume ratio determination in static expansion systems by means of a spinning rotor gauge, *Vacuum*, 52 (1999), 491–499
- [4] K. Jousten, Temperature relaxation of argon and helium after injection into a vacuum vessel, *Vacuum*, 45 (1994), 1205–1208
- [5] W. Jitschin, High-accuracy calibration in the vacuum range 0.3 Pa to 4000 Pa using the primary standard of static gas expansion, *Metrologia*, 39 (2002), 249–261
- [6] R. G. Livesey, Solution methods for gas flow in ducts through the whole pressure regime, *Vacuum*, 76 (2004), 101–107, doi: 10.1016/j.vacuum.2004.05.015
- [7] Handbook of Vacuum Technology, 2nd edition, K. Jousten (editor), Wiley-VCH Verlag Co. KGaA, Weinheim (2016), ISBN 978-3-527-41338-6
- [8] K. W. Elliott and P. B. Clapham, NPL report MOM, 28 (1978)
- [9] Th. Bock, H. Ahrendt and K. Jousten, Reduction of the uncertainty of the PTB vacuum pressure scale by a new large area non-rotating piston gauge, *Metrologia*, 46 (2009), 389–386
- [10] F. J. Redgrave, A. B. Forbes and P. M. Harris, A discussion of methods for the estimation of volumetric ratios determined by multiple expansions, *Vacuum*, 53 (1999), 159–162
- [11] J. Fremerey, The Spinning Rotor Gauge, *Journal of Vacuum Science & Technology A: Vacuum, Surfaces, and Films*, 3 (1985), 1715–1720